Energy Materials

Supplementary Materials

Hydrophobic modification regulates the water microenvironment at the interface of Cu-based materials to promote E-CO_2RR

Ke-Xian Li[1,2,3], Yan-Xin Chen[1,2,3,4,5,*], Hao-Yan Shi[1,2,5], Hai-Long Wang[1,2,5], Yi-Hong Wu[1,2,5], Xiao-Wei Wu[1,2], Song-Ling Wang[1,2], Yang Ding[6], Ai-Zhong Jia[7,*], Paolo Fornasiero[8,*], Can-Zhong Lu[1,2,3,4,5,*]

[1]State Key Laboratory of Structural Chemistry, Fujian Science & Technology Innovation Laboratory for Optoelectronic Information of China, and Fujian Institute of Research on the Structure of Matter, Chinese Academy of Sciences, Fuzhou 350108, Fujian, China.

[2]Xiamen Key Laboratory of Rare Earth Photoelectric Functional Materials, Xiamen Institute of Rare-earth Materials, Xiamen 361021, Fujian, China.

[3]Fujian College, University of Chinese Academy of Sciences, Fuzhou 350002, Fujian, China.

[4]College of Chemistry, Fuzhou University, Fuzhou 350116, Fujian, China.

[5]College of Chemistry University of Chinese Academy of Sciences, Beijing 100049, China.

[6]College of Materials and Environmental Engineering, Hangzhou Dianzi University, Hangzhou 310018, Zhejiang, China.

[7]Hebei Provincial Key Laboratory of Green Chemical Technology and High Efficient Energy Saving, School of Chemical Engineering and Technology, Hebei University of Technology, Tianjin 300401, China.

[8]Department of Chemical and Pharmaceutical Sciences, ICCOM-CNR (Institute of Chemistry of Organometallic Compounds, Consiglio Nazionale delle Ricerche), and INSTM (National Interuniversity Consortium of Materials Science and Technology), Trieste Research Unit, University of Trieste, Trieste 34127, Italy.

*Correspondence to: Prof. Yan-Xin Chen, Prof. Can-Zhong Lu, State Key Laboratory of Structural Chemistry, Fujian Science & Technology Innovation Laboratory for Optoelectronic Information of China, and Fujian Institute of Research on the Structure of Matter, Chinese Academy of Sciences, Fuzhou 350108, Fujian, China. E-mail: yanxinchen@fjirsm.ac.cn; czlu@fjirsm.ac.cn; Prof. Ai-Zhong Jia, Hebei Provincial Key Laboratory of Green Chemical Technology and High Efficient Energy Saving, School of Chemical Engineering and Technology, Hebei University of Technology, Tianjin 300401, China. E-mail: azhjia@hebut.edu.cn; Prof. Paolo Fornasiero, Department of Chemical and Pharmaceutical Sciences, ICCOM-CNR (Institute of Chemistry of Organometallic Compounds, Consiglio Nazionale delle Ricerche), and INSTM (National Interuniversity Consortium of Materials Science and Technology), Trieste Research Unit, University of Trieste, Trieste 34127, Italy. E-mail: pfornasiero@units.it

1. Experimental details

1.1 Material Characterization

The microstructure of the samples was observed using SEM at an acceleration voltage of 15 kV (SEM, Apreo S, Thermo Fisher Scientific, Waltham, MA, USA); subsequent TEM, HRTEM, and SAED (TEM, FEI-TALOS-F200X**,** Thermo Fisher, Waltham, MA, USA) characterization was performed at an acceleration voltage of 200 kV to investigate the fine structure, size distribution, and elemental composition of the samples. The elemental composition and concentration of the samples were determined using an energy-dispersive X-ray spectrometer (EDS; Hitachi SU1510 and Oxford X-MAX 80T). XRD data were acquired using an X-ray diffractometer (Cu Kα radiation, scanning range 20°-80°, MiniFlex600, Thermo Fisher Scientific, Japan) to determine the crystal structure of the samples. An X-ray photoelectron spectrometer (XPS, Thermo Scientific K-Alpha, Waltham, MA, USA) was used to characterize the elemental composition and chemical state of the sample surfaces. A Fourier transform infrared spectrometer (Nicolet iS 50 Thermo Fisher, Waltham, MA, USA) was used to analyze changes in the functional groups of the catalyst.

1.2 E-CO_2RR Testing Experiment

The E-CO_2RR tests were conducted at room temperature. A catalyst slurry was prepared, and the catalyst was applied to carbon paper (1.5 × 1.5 cm) via spraying, with a catalyst loading of 1 mg/cm^2. The slurry was prepared by mixing 10 μL of Nafion with 3 mL of isopropanol and sonicating for 10 minutes, followed by the addition of 2.25 mg of catalyst ((111) Cu_2O) and sonication for 30 minutes. A gas diffusion electrode (GDE, test area 1 × 1 cm^2) and a nickel foam were used as the cathode and anode, respectively, with Hg/HgO (1M KOH) serving as the reference electrode, and all components were assembled into a flow cell. The gap between the GDE and the anion-exchange membrane (FAA-3-PK-75) forms the cathode compartment, which is filled with 1 M KOH; the anode compartment is also filled with 1 M KOH. A peristaltic pump is used to circulate cathode and anode solutions within their respective compartments at flow rates of 60 rpm (cathode compartment) and 250 rpm (anode compartment). Prior to testing, high-purity CO_2 (99.995%) is continuously bubbled into the cathode electrolyte for 20 minutes before testing begins (25 mL/min).

2. E-CO_2RR Testing

2.1 Neutral Conditions Test

The tests were carried out under room temperature conditions. A prepared gas diffusion electrode (GDE, with a test area of 1×1 cm^2) and a titanium felt (Ir/Ta coated) were used as the cathode and anode, respectively, and Ag/AgCl (saturated KCl) was used as the reference electrode in a flow electrolytic cell (Purchased from Gaoss Union(Tianjin) Photoelectric Technology Co., Ltd).

The gap between the GDE and the membrane serves as the cathode electrolyte compartment, which is filled with 1 M KOH. The anode electrolyte chamber is filled with 1 M KOH. The cathode and anode electrolyte chambers are separated by a proton exchange membrane (Nafion N115). Prior to testing, a 1 M KOH solution

saturated with carbon dioxide (pH = 7.6) was prepared by continuously passing high-purity carbon dioxide (99.995%) through the cathode electrolyte for 20 minutes. During the experiment, two peristaltic pumps were used to facilitate continuous circulation of the electrolyte in the cathode and anode compartments, thereby ensuring continuous renewal of the electrolyte on the GDE surface. The flow rates of the cathode and anode electrolytes were 11 mL/min and 42 mL/min, respectively. CO_2 gas was delivered directly to the cathode gas chamber at a flow rate of 25 mL/min (standard cubic centimeters per minute, "sccm"); to ensure experimental accuracy, a mass flow meter (Sevenstar Flow Meter, Sevenstar) was used to monitor the inlet flow rate. Prior to conducting electrochemical CO_2 reduction tests, all gas diffusion electrodes were preconditioned for 15 minutes at a current of 250 mA. CO_2RR experiments were conducted on a Squidstat Plus electrochemical workstation (Admiral Instruments). H-type cells were pretreated for 15 minutes at a reduction potential of -0.95 V (relative to RHE) prior to electrochemical testing. Other electrochemical tests (such as cyclic voltammetry (CV) tests) were also performed. The applied potentials were converted to reference potentials relative to RHE using the following formula:

$$E_{RHE} = E_{Ag/AgCl} + 0.0592 \times pH + 0.1976 - iR \qquad (1)$$

Where, $E_{Ag/AgCl}$=0.1976 V *vs.* SHE (25 °C), i is the total current density, and the solution resistance R was determined by electrochemical impedance spectroscopy in the frequency range of 100 kHz to 1 Hz, with a value of 2.5 ohms. Except for some test data related to the flow cell, specifically those in Figure 5a-l, no iR correction was performed on other potentials.

2.2 Product analysis

The gas phase products were quantified by gas chromatography (GC9790 Plus, FULI instruments). H_2, CO, CH_4, and C_2H_4 were quantified by a thermal conductivity detector (TCD) and flame ionization detector (FID), respectively. The *FE* of the gas products was calculated using the following equation:

$$FE_g(\%) = \frac{Fn_gVx_g}{j} \times 100 \qquad (2)$$

In this equation, x_g represents the mole fraction of the product, n_g denotes the number of electrons transferred, *V* signifies the outlet gas flow rate, *j* represents the total current, and F is the Faraday constant (96485 C·mol^{-1}).

For quantitative analysis, all liquid phase products were passed through a 500 MHz NMR spectrometer (Bruker Avance 500 MHz). Dimethyl sulfoxide (DMSO) was added as an internal standard in the NMR assay. After a constant potential or constant potential after an electrolysis time t, 0.5 mL of the electrolyte solution was removed as a sample for quantitative analysis of CO_2 products in the liquid phase of electrochemical reduction. The method was as follows: 0.5 mL of the liquid to be analyzed was homogeneously mixed with 0.1 mL D_2O, and 0.1 μL of DMSO was homogeneously mixed in an NMR tube to be tested. The FE of the liquid products (FE_l)was calculated using the following equation:

$$FE_l(\%) = \frac{Fn_lVc_l}{j \times t} \times 100 \qquad (3)$$

In this context, F represents the Faraday constant (96485 C·mol^{-1}), *j* denotes the total current density, n_l signifies the number of electrons transferred to generate the corresponding product l, *t* stands for the total reaction time, *V* is the volume of electrolyte, and c_l represents the concentration of the l product.

The half-cell energy conversion efficiency (CEE, also known as the cathodic energy efficiency) is calculated by the following formula:

$$CEE_i(\%) = \frac{(1.23 - E_i) \times FE_i}{1.23 - E} \qquad (4)$$

Where, E_i refers to the thermodynamic potential of product i, the E_i of ethylene is 0.08 V *vs.* RHE, E (V *vs.* RHE) represents the applied potential, and FE_i denotes the calculated Faraday efficiency of product i.

The yield of the products obtained from the carbon dioxide reduction process is calculated using the following formula:

$$Yield_i = \frac{X_i \times (R \times 60) \times 0.001}{V_m \times m} \quad (5)$$

Among them, X_i represents the volume fraction of product i in the gas mixture after the reaction. R represents the flow rate of the reactant CO_2 (with the unit of sccm). V_m represents the molar volume of gas, which is 24.47 mol/L at 20 ℃. m represents the mass of the catalyst involved.

3. ATR-SEIRAS testing

A polycrystalline Au film was chemically deposited on the reflective surface of a semi-cylindrical Si column before testing, and the Au film was prepared using a chemical plating technique to enhance the IR signal. The steps were as follows: first, the Si column was polished with 0.3 μm alumina slurry until the reflective surface was completely hydrophobic, and then the Si column was rinsed with water; then the Si column was polished with 0.05 μm silica slurry until the reflective surface was completely hydrophobic, and then the Si column was rinsed thoroughly with water. In order to remove the residual slurry, the Si column was sonicated in ethanol and ultrapure water sequentially five times, each for 1 minute. After ultrasonic cleaning, the prism reflective surface was immersed in NH_4F for 90 seconds to remove the oxide layer and form a terminal hydrogen surface to improve the adhesion of the Au film. The Si surface was then immersed in a mixture of Au plating solution and HF solution at 50 ℃ for about 3 min. The quality of the film was checked using a multimeter where the desired resistance on the film was between 5-20 ohms.

In-situ ATR-SEIRAS experiments used an infrared spectrometer (Nicolet iS50 FTIR, Thermo Fisher Scientific) and a SPEC-II (Shanghai Yuanfang Technology Co., Ltd) reflectance infrared optical path system. The data were acquired with a spectral resolution of 4 cm^{-1}. The experiments used a customized infrared spectroscopic reaction cell (SPECEL-I, internal reflectance spectroscopic cell, Shanghai Yuanfang Technology Co., Ltd). After assembling the electrolytic cell, the gold-plated silicon column was pre-cleaned by adding 0.5 M H_2SO_4 electrolyte. After cleaning, the gold film on the surface of the gold-plated silicon column was rinsed with water several

times. Next, the sample to be tested (2 mg·mL^{-1}) was drop-coated on the cleaned gold film, and the sample was dried using an infrared oven during the drop-coating process. The electrolytic cell was reassembled again, and then the surface of the gold-plated silicon column with the sample was used as the working electrode for ATR-SEIRAS measurements, and a continuously CO_2-saturated 1 M KOH electrolyte was used as the electrolyte for testing. Potential-dependent sample spectra were collected using an average of 32 scans with a test potential interval of 0 V to -1.3 V (*vs.* RHE, no iR correction).

4. Theoretical calculations

All the DFT calculations were conducted based on the Vienna Ab initio Simulation Package (VASP) [1-2]. The exchange-correlation potential was described by the Perdew–Burke–Ernzerhof (PBE) generalized gradient approach (GGA) [3]. The electron-ion interactions were accounted by the projector augmented wave (PAW) [4]. All DFT calculations were performed with a cut-off energy of 500 eV, and the Brillouin zone was sampled using a 3 × 3 × 1 k-point grid. To accurately model the surface and avoid spurious interactions between periodic images, a vacuum layer exceeding 15 Å was introduced along the direction perpendicular to the surface (the c-axis). The energy and force convergence criteria of the self-consistent iteration were set to 10^{-5} eV and 0.02 eV Å^{-1}, respectively. DFT-D3 method was used to describe van der Waals (vdW) interactions[5].

The Gibbs free energy changes (ΔG) of the reaction are calculated using the following formula:

$$\Delta G = \Delta E + \Delta \mathrm{ZPE} - T\Delta S + \Delta G_{\mathrm{U}} + \Delta G_{\mathrm{pH}} \qquad (6)$$

where ΔE is the difference of electron energies calculated by DFT; ΔZPE and ΔS are the changes of zero-point energy and entropy, respectively, which are obtained from vibrational frequencies. T is the temperature (298.15 K). $\Delta G_{\mathrm{U}} = -eU$, where U is the applied electrode potential. $\Delta G_{\mathrm{pH}} = k_{\mathrm{B}}T \times \ln 10 \times \mathrm{pH}$, where k_{B} is the Boltzmann

constant.

5. Figures and Tables

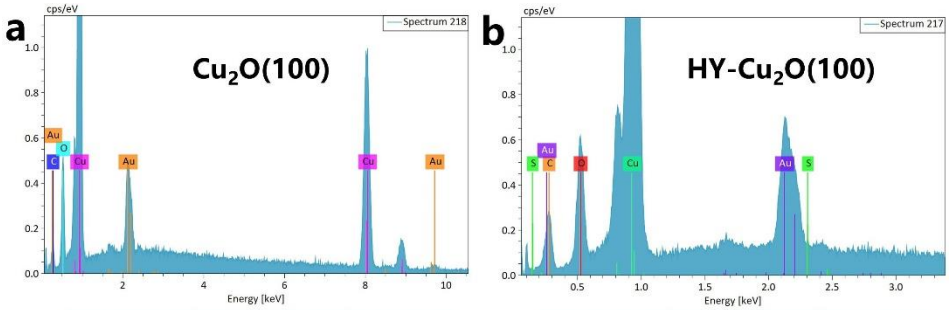

c

element	normalized quality(%)	atomic mass(%)
Cu	83.59	72.73
O	4.56	15.72
C	1.96	8.98
Au	9.90	2.77
	100.00	100.00

d

element	normalized quality(%)	atomic mass(%)
Cu	78.27	59.14
O	5.74	17.23
S	0.11	0.16
C	5.22	20.87
Au	10.66	2.6
	100.00	100.00

Figure S1. (a) EDS characterization results of Cu_2O (100) and (b) HY-Cu_2O (100). (c) The relative elemental content of Cu_2O (100) and (d) HY-Cu_2O (100).

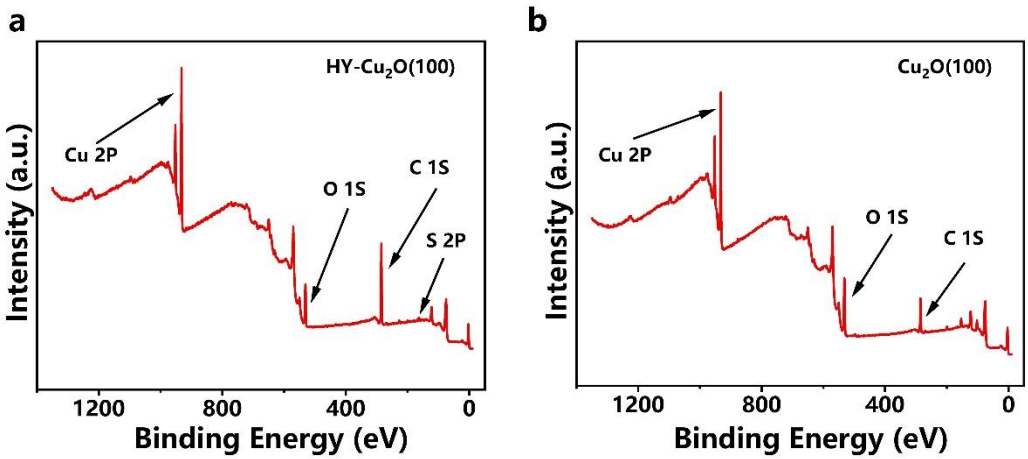

FigureS2. XPS spectra of (a-b) HY-Cu_2O (100) and Cu_2O (100).

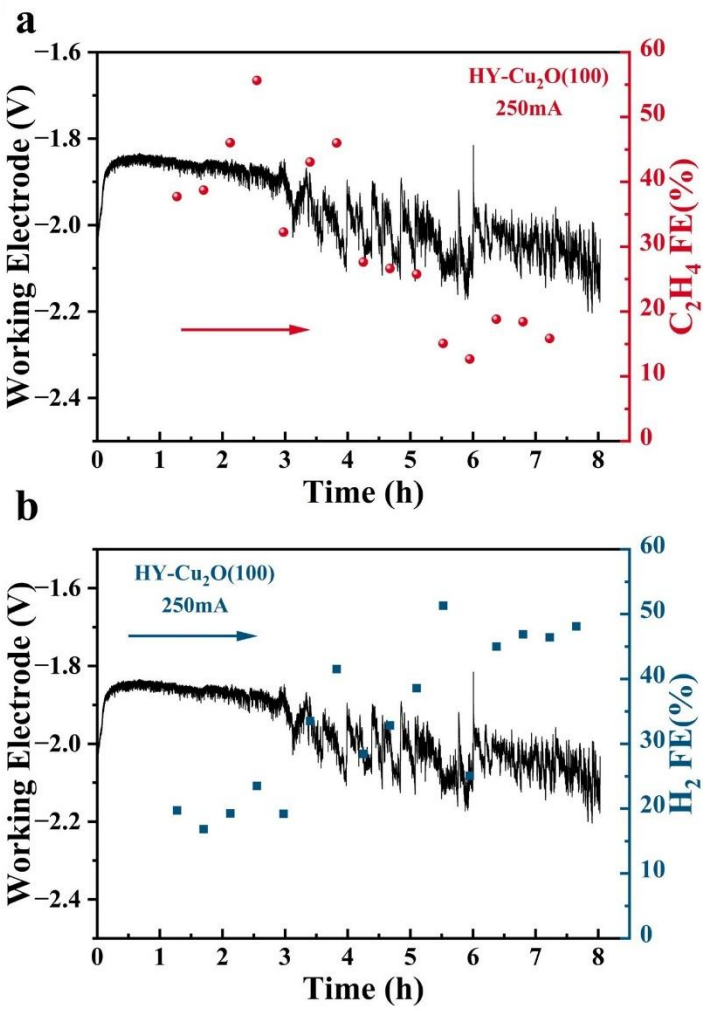

FigureS3. Stability testing of HY-Cu_2O (100). (a) FE plot for C_2H_4. (b) FE plot for H_2 (current: 250 mA, CO_2 flow rate: 25 sccm).

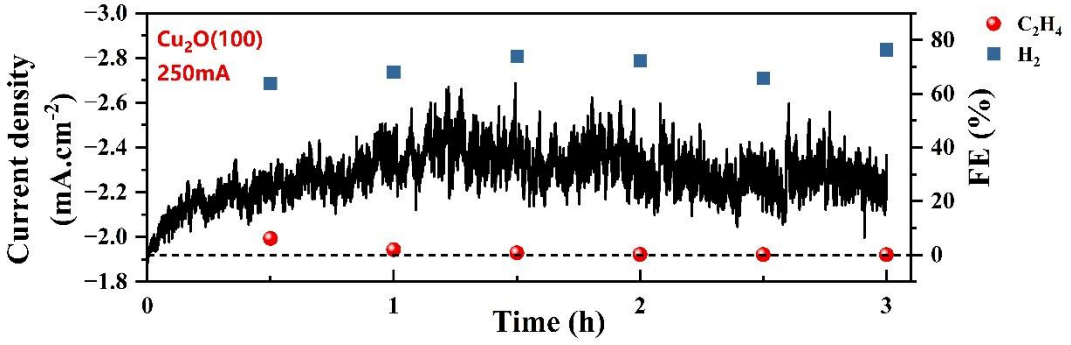

FigureS4. Stability testing of Cu_2O (100). (current: 250 mA, CO_2 flow rate: 25 sccm).

FigureS5. Structures of the reaction intermediates (*CO, *COH, and O*C*COH) of asymmetric HB-H_2O on a Cu_2O (100) electrode.

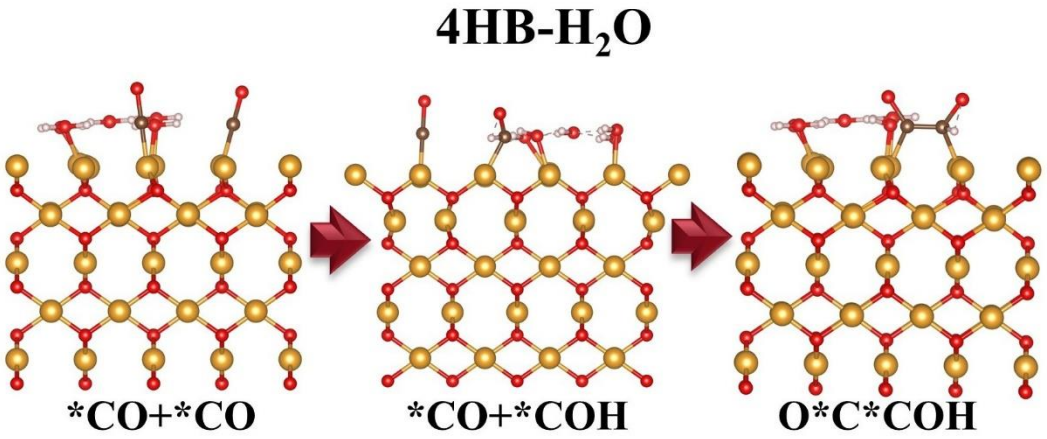

FigureS6. Structures of the reaction intermediates (*CO, *COH, and O*C*COH) of 4HB-H_2O on a Cu_2O (100) electrode.

Table S1. Latest Research Report on Electrochemical CO_2 Reduction Using Hydrophobically Modified Catalyst

Electrolyte	Catalysts	j_{total} ($mA \cdot cm^{-2}$)	Ethylene FE (%)	References
1 M KOH	HY-Cu_2O (100)	250	C_2H_4 (45.2)	This work
1 M KOH	OD-Cu-HIL PNPs Pulsed methods	600	C_2H_4 (53)	*J. Am. Chem. Soc.* 2025.[6]
0.5M $KHCO_3$	Au NWs-P1	120	C_2H_4 (58)	*J. Am. Chem. Soc.* 2025.[7]
1 M KOH	P-GDE	800	C_2H_4 (33.5)	*Nano Res.* 2021.[8]
1 M KOH	SnS_2 + PVDF 50	150	HCOOH (93)	*Green Chem.*,2025[9]
0.5 M $KHCO_3$	Au(-CB[6]) NPs	8.1	CO (97)	*Journal of Alloys and Compounds,* 2024[10]
0.5 M $KHCO_3$	Co-Terpy-RF	10	CH_4 (80)	*Nature Chem,* 2024[11]

References

[1] G. Kresse, J. Hafner, Ab Initio molecular Dynamics for Liquid Metals, *Phys. Rev. B* 47 (**1993**) 558-561.

[2] G. Kresse, J. Hafner, Ab initio molecular-dynamics simulation of the liquid-metalamorphous-semiconductor transition in germanium, *Phys. Rev. B Condens. Matter Mater. Phys*. 49 (**1994**) 14251–14269.

[3] J. P. Perdew, K. Burke, M. Ernzerhof, Generalized Gradient Approximation Made Simple. *Phys. Rev. Lett.* 77 (**1996**) 3865-3868.

[4] G. Kresse, D. Joubert, From ultrasoft pseudopotentials to the projector augmented-wave method, Phys. Rev. B Condens. *Matter Mater. Phys.* 59 (**1999**) 1758–1775.

[5] S. Grimme, J. Antony, S. Ehrlich, H.A. Krieg, Consistent and accurate ab initio parametrization of density functional dispersion correction (DFT-D) for the 94 elements H-Pu, *J. Chem. Phys.* 132 (2010), 154104.

[6] R. H. Chen, Q. Wu, J. C. Zhu, et al.,"Hydrophobic Ionic Liquid Engineering for Reversing CO Intermediate Configuration toward Ampere-Level CO_2 Electroreduction to C_{2+} Products", *Journal of the American Chemical Society* 2025, 147, 7921. https://doi.org/10.1021/jacs.4c18508

[7] Y. L. Chen, K. C. Wei, H. Y. Duan, et al.,"N-Heterocyclic Carbene Polymer-Stabilized Au Nanowires for Selective and Stable Reduction of CO_2", *Journal of the American Chemical Society* 2025, 147, 14845. https://doi.org/10.1021/jacs.5c04742

[8] L. Y. Xue, X. F. Wu, Y. W. Liu, et al.,"Hydrophobic 1-octadecanethiol functionalized copper catalyst promotes robust high-current CO_2 gas-diffusion electrolysis", *Nano Research* 2022, 15, 1393. https://doi.org/10.1007/s12274-021-3675-6

[9] Z. Dong, Y. Jia, Z. Wang, et al.,"Regulating the hydrophobic microenvironment of SnS_2 to facilitate the interfacial CO_2/H_2O ratio towards pH-universal electrocatalytic CO_2 reduction", *Green Chemistry* 2025, 27, 5498. https://doi.org/10.1039/d5gc00635j

[10] T. Ma, L. Qiu, Y. Tao, et al.,"Ligand dominating the catalytic performance of cucurbit[6]uril modified gold nanoparticles for electrocatalytic CO_2 reduction", *Journal of Alloys and Compounds* 2024, 979, 173477.

https://doi.org/10.1016/j.jallcom.2024.173477

[11] M. McKee, M. Kutter, Y. Wu, et al.,“Hydrophobic assembly of molecular catalysts at the gas–liquid–solid interface drives highly selective CO_2 electromethanation”, *Nature Chemistry* 2024, 17, 92. https://doi.org/10.1038/s41557-024-01650-6